RESEARCH ARTICLE



Future transitions from a conifer to a deciduous-dominated landscape are accelerated by greater wildfire activity and climate change in interior Alaska

Shelby A. Weiss · Adrienne M. Marshall · Katherine R. Hayes · Dmitry J. Nicolsky · Brian Buma · Melissa S. Lucash

Received: 9 March 2023 / Accepted: 12 July 2023 / Published online: 26 July 2023 © The Author(s), under exclusive licence to Springer Nature B.V. 2023

Abstract

Context In interior Alaska, increasing wildfire activity associated with climate change is projected to continue, potentially altering regional forest composition. Conifers are emblematic of boreal forest; however, greater frequency and severity of wildfires has been found to favor broadleaf-deciduous species in numerous studies.

Objectives This study examines potential shifts in forest type in interior Alaska and how shifts may be impacted by recurring wildfires under future climate change.

Methods A spatially-explicit forest landscape model, LANDIS-II, was used to simulate forest succession and wildfire over a 380,400-hectare landscape

Supplementary Information The online version contains supplementary material available at https://doi.org/10.1007/s10980-023-01733-8.

S. A. Weiss · M. S. Lucash Department of Geography, University of Oregon, 1251 University of Oregon, Eugene, OR 97403, USA

Present Address: S. A. Weiss (⋈)

The National Great Rivers Research and Education Center, 1 Confluence Way, East Alton, IL 62024, USA e-mail: saweiss@lc.edu

A. M. Marshall

Hydrologic Sciences and Engineering Program, Colorado School of Mines, 1500 Illinois St, Golden, CO 80401, USA under historic and future (RCP 8.5) climate. Wildfire was modeled using the SCRPPLE fire extension and vegetation growth, belowground carbon, hydrologic, and permafrost dynamics were modeled with the DGS succession extension. The relative importance of drivers of forest type change away from black spruce was quantified using random forest models for areas on the landscape experiencing different numbers of wildfires.

Results Greater frequencies of fire activity were associated with shifts in conifer-dominant areas to broadleaf-deciduous, which climate change accelerated. Vegetation transitions were most strongly influenced by percent tree mortality from the most recent wildfire. Starting deciduous fraction and proximity of mature black spruce to a site pre-fire were also influential, indicating pre-fire composition and context modified the effect of vegetation shifts.

K. R. Hayes Cary Institute of Ecosystem Studies, 2801 Sharon Turnpike, Millbrook, NY 12545, USA

D. J. Nicolsky
Geophysical Institute, University of Alaska Fairbanks,

2156 Koyukuk Drive, Fairbanks, AK 99775, USA

B. Buma

Environmental Defense Fund, 2060 Broadway St, Ste 300, Boulder, CO 80302, USA



Conclusions These results underscore how shifts in forest type may occur in a nonlinear manner in this region as the landscape experiences pressure from climate change and forests are subject to complex interactions between wildfire, climate, belowground processes, and the arrangement of forest communities.

Keywords Boreal forest · Forest landscape simulation · Random forest · Wildfire · Climate change

Introduction

The boreal forest is the most extensive terrestrial biome on Earth, covering ~29% of the Earth's surface. This biome is defined by its cold winters and relatively low tree diversity, dominated primarily by evergreen conifers. However, it is warming more rapidly than other biomes—approximately two to three times as fast as the global mean (Taylor et al. 2013). Warming is causing a host of changes in boreal ecosystems, including extensive thawing of permafrost (Nelson et al. 2001), changes in hydrology (Rowland et al. 2010), wildfires (Flannigan et al. 2009), insects (Volney and Fleming 2000), and vegetation (Johnstone et al. 2010b). In interior Alaska, there is growing concern that black spruce (Picea mariana) forest communities will undergo a state shift from spruce- to broadleaf deciduous-dominance due to climate-driven changes in fire regime (Johnstone et al. 2010b; Shenoy et al. 2011). Black spruce has been the dominant forest type in interior Alaska for the past 5000–6000 years (Lynch et al. 2002; Higuera et al. 2009) via several mechanisms: the serotinous cones of black spruce which allow for prolific seed dispersal and rapid regeneration post-fire (Zasada et al. 1992), large seeds, and adventitious roots. In mature black spruce stands, slow decomposition and slow nutrient turnover promote and maintain moist, cool soils, allowing thick soil organic layers to develop (Johnstone et al. 2016). This thick layer inhibits seedling establishment for most tree species in the region, however, the relatively larger size of black spruce seeds allows them to regenerate on these seedbeds (Johnstone and Chapin 2006b; Greene et al. 2007; Johnstone et al. 2010a). The adventitious roots of mature black spruce also make it possible to access water and nutrients from within the organic layer and survive atop near-surface permafrost (van Cleve et al. 1983). These competitive advantages enable early establishment of spruce at the exclusion of deciduous competitors and continued dominance as stands mature. These competitive mechanisms enable black spruce to be self-replacing over long fire-free periods (fires recurring every 70–130 years, Johnstone et al. 2010a, b).

In recent decades, annual area burned, fire season length, and fire severity have increased while fire return intervals have decreased; these changes in Alaska's fire regime are projected to continue (Flannigan et al. 2009; Kasischke et al. 2010). High-severity fires promote persistent shifts from black spruce to deciduous dominance via more complete (depth and extent) consumption of the soil organic layer (Johnstone and Chapin 2006b; Johnstone et al. 2010b; Shenoy et al. 2011) and black spruce seedbanks. Multiple fires with less recovery time prevent the soil organic layer from building up between fires, such that when areas reburn, less residual soil organic layer remains and it is more readily consumed, exposing mineral soil (Johnstone et al. 2016; Hoy et al. 2016; Hayes and Buma 2021; Shabaga et al. 2022). In addition, shorter fire return intervals reduce seed availability of black spruce for post-fire regeneration. Black spruce does not start producing cones consistently until around 30 years of age and often do not maximize seed productivity until much later (e.g., > 100 years; Buma et al. 2013; Viglas et al. 2013) so repeat fires, or 'reburns', within 30-50 years extirpate black spruce post-fire seed regeneration (Johnstone and Chapin 2006a). While black spruce are semi-serotinous and burned mature stems act as a seed source within fire scars, nearby reserves of unburned trees are an important contributor to total viable seed rain, particularly when high severity fires compromise the aerial seed bank (Johnstone et al. 2009). When a new fire burns into a previously burned area with relatively young black spruce stand and the distance to the burn perimeter exceeds the seeding distance (80 m for an individual black spruce, Burns and Honkala 1990), opportunities for reestablishment within burn perimeters are limited (Johnstone et al. 2016). As such, the size, shape and overlap of individual fires influence future black spruce reproductive success within reburns.

In addition to neighborhood effects being an important factor in reestablishment post-disturbance,



local site conditions can buffer climate and wildfire impacts on regeneration. Past work has found that higher soil moisture is associated with greater reproductive success and growth following a fire in black spruce forests; lesser consumption of the soil organic layer and a corresponding greater regeneration of black spruce has been observed following two shortinterval fire events in wetter, lowland areas, compared to drier upland sites (Hayes and Buma 2021). Patterns in annual primary productivity over time also diverge between dry and mesic sites, increasing linearly on mesic sites over time, while peaking mid-succession before declining on drier sites where deciduous species and willow (Salix spp.) become dominant midway through succession (Mack et al. 2008). Similarly, Johnstone et al. (2010a, b) found that sites with higher moisture initially had greater densities of black spruce and greater black spruce re-establishment post-fire.

Several simulation modeling studies from interior Alaska have examined the potential for shifts in dominant vegetation type, making significant progress toward improving our predictive capacity in North American boreal forest ecosystems. Past work has commonly predicted a greater relative landscape-scale deciduous dominance triggered by climate-driven fire regime change; however, several areas remain unexplored. Existing large-scale modeling efforts have largely operated at coarse resolutions which cannot capture site and neighborhood level mechanisms (e.g., 1 km² or larger; Mann et al. 2012; Mekonnen et al. 2019) and representation of forest communities has been limited to the functional group-level or to tree species (Mann et al. 2012; Foster et al. 2019; Mekonnen et al. 2019; Hansen et al. 2021). Nonetheless, climatic variables may influence interspecific dynamics between species throughout succession, thus including non-tree species in modeling efforts is important to better understand their role. Past modeling efforts have also largely lacked spatial interactivity (i.e., allowing processes to overlap spatially, tracking their cumulative effects; Foster et al. 2019; Hansen et al. 2021), and so do not capture how impacts of climate change and wildfire on vegetation composition trajectories may be mediated by spatial contagion effects from the surrounding landscape. This study uses the DAMM-MCNiP-GIPL-SHAW (henceforth 'DGS') extension to LANDIS-II (Lucash et al. 2023), a new succession extension for the forest landscape model which integrates the vegetation dynamics of the Net Ecosystem Carbon and Nitrogen (NECN) LANDIS-II extension with soil carbon dynamics of the Dual Arrhenius Michaelis-Menton-Microbial Carbon and Nitrogen Physiology (DAMM-McNIP) model, hydrology of Simultaneous Heat and Water (SHAW) model and permafrost dynamics of the Geophysical Institute Permafrost Laboratory (GIPL) model v2.0 within a spatiallyexplicit framework that interfaces with an existing wildfire extension to simulate ignitions, spread, and severity. DGS simulates the growth, mortality, and reproduction of vegetation, while also simulating energy and water fluxes (e.g., snow depth, evapotranspiration, soil moisture) and temperature at multiple levels in the canopy and up to 75 depths in the soil. By applying DGS in this context, we explore how climate change and increasing fire frequency alter species composition, dominance, and spatial arrangement, and quantify the relative influences of fire history, seed source patterns, climate, and soil conditions on future post-fire successional trajectories.

Materials and methods

Study area

The modeling domain for this study consists of a 380,400-hectare landscape in interior Alaska, composed of 4-ha grid cells. The specific area was chosen for its proximity to field sites where reference data were located, used in validating the performance of the DGS extension. The study landscape is situated within the intermontane basin and plateau region of Alaska; it features rolling hills intersected with river valleys (Begét et al. 2006). The elevation within the domain ranges from 93 to 950 m, with a mean elevation of 331.4 m (SD=140.01 m). The region falls within the discontinuous permafrost zone; cool and wet lowland areas, as well as north facing slopes, are often underlain with permafrost (Stralberg et al. 2020). The study area is relatively flat with a mean slope of 6.3 degrees (SD=5.0 degrees), though the maximum slope is 36.13 degrees. Between 1992 and 2015, the study area experienced 1.05 wildfires per year (SD=1.12) with an average fire size of 3,795 hectares (SD = 9.872.60 ha) and a fire rotation of 119 years (Short 2023).



LANDIS-II model

LANDIS-II (v. 7), an open-source spatially explicit forest landscape simulation model (Scheller et al. 2007) was used to simulate successional dynamics and wildfire over the study landscape. LANDIS-II is modular, with a variety of extensions available to represent ecosystem processes such as forest growth and disturbances such as wildfire, offering flexibility in the level of complexity captured by the model. It operates on grid cells that contain speciesage cohorts, and these cohorts may grow and compete with one another within a cell over time based on species-specific attributes including longevity, reproductive ages, shade tolerance, seeding distances, and post-fire regeneration strategies (e.g., serotiny and resprouting). Individual cells may contain multiple cohorts of each species, allowing for complex species and age structures. The individual processes captured within LANDIS-II extensions are typically calibrated using reference data—however, simulations have no single successional pathway once executed since processes such as regeneration (e.g., seed dispersal and resprouting) and disturbances (e.g., fire) are stochastic and interact spatially across the landscape.

Description of DGS extension

This study used the DGS extension to LANDIS-II (Lucash et al. 2023), which simulates vegetation succession, hydrology, carbon and nitrogen dynamics, and ground temperature across a large range of depths. The DGS extension was designed specifically for use in boreal regions, capturing the belowground water and temperature dynamics unique to high latitude systems. Including belowground processes when modeling boreal ecosystems is important as soil moisture is influenced by the presence of permafrost and soil moisture affects the freeze/thaw dynamics within the soil (Fisher et al. 2016). DGS couples SHAW model and the GIPL heat flow model within the LANDIS-II framework. The SHAW model is a physically-based model which simulates the vertical transfer of heat, water, and solutes at up to 75 user-defined depths down to 30 m as influenced by live and dead vegetation and snow. SHAW captures evapotranspiration, snow accumulation and ablation, and surface runoff and infiltration (Flerchinger 2000). The GIPL model receives the total water content values from SHAW, simulates ground temperature dynamics from the ground/snow surface to the maximum soil depth, and outputs temperature at user defined depths, as well as active layer and talik thicknesses. The GIPL model solves a nonlinear heat equation with phase change in the porous material and was applied to simulate permafrost dynamics across a variety of contexts in Alaska (Marchenko et al. 2008; Nicolsky et al. 2017).

Within the DGS extension, climate zone, vegetation type, topographic information, and time-sincefire are used to assign cells at each time step to a specific temperature-hydrology unit ('THU''; Lucash et al. 2023). Each THU has specific sets of SHAW and GIPL input parameters specifying thermal and hydrological properties of the soil column associated with that given THU. Based on the THU assigned at each timestep in combination with climate data inputs, GIPL computes a soil temperature profile (Nicolsky et al. 2017) which is used to inform the SHAW lower soil temperature boundary condition. This information is used in combination with THU assignment to compute the soil moisture and temperature at each depth in the soil profile (Flerchinger 2000). Soil moisture and temperature information are then shared with the vegetation in DGS, aggregated to two depths: from 10 cm to the surface to reflect the ability of adventitious roots to acquire surficial soil moisture, and from 10 cm to a species-specific rooting depth for all tree and shrub species (Lucash et al. 2023). DGS uses these estimates of soil moisture and temperature to quantify the water and temperature limitations to species cohort growth. Within the DGS extension, growth is simulated monthly based on life-history attributes which are specified for each species as well as temperature, age, competition, water availability, nitrogen availability, and disturbances (Lucash et al. 2023; Scheller et al. 2011). Regeneration is influenced by species attributes, light, and water availability (Scheller et al. 2011). Soil Carbon (C) and Nitrogen (N) dynamics rely upon the DAMM-MCNiP model (Abramoff et al. 2017), which simulates seven measurable soil pools (soil organic C, dissolved organic C, dissolved organic N, microbial biomass C, microbial biomass N, and extracellular enzymes) which are sensitive to soil moisture, soil temperature, oxygen concentrations, and substrate CN stoichiometry.



Vegetation inputs

To map the initial vegetation composition for the simulation landscape, we used U.S. Forest Service Forest Inventory and Analysis data (FIA) from the Tanana region surveys in interior Alaska (USDA-Forest Service 2018) in combination with the Alaska Center for Conservation Science Mosaic Landcover Map of Alaska (Alaska Center for Conservation Science 2017). Six tree species, three shrub genera, and three moss functional types were initiated on the landscape (Appendix A). Following the methodology of Lucash et al. (2019), FIA plots were associated with cover types from a detailed landcover map (Alaska Center for Conservation Science 2017), an elevation map (USGS 2020a), and a climate region map (see below). Tree ages within FIA plots were estimated using site index curves (Carmean et al. 1989). Then, species-age cohort data from FIA plots were imputed within each cell on the landscape according to which plots most closely corresponded with site characteristics (e.g., elevation categories, hierarchical land cover type classifications) and stand age (estimated from a fire history dataset; FRAMES 2016), with priority given to plots that matched a given cell most precisely (i.e. most detailed land cover type, closest in value to stand age and elevation). When multiple FIA plots equally well matched grid cell site characteristics, a random plot was selected from the pool of potential matches. The FIA database did not contain biomass information for shrub species but included percent cover by height class for each plot, so biomasses were estimated based on percent cover, height class, and associated stand ages. We developed linear models relating shrub biomasses at specific height classes and associated percent cover using Bonanza Creek LTER data archive datasets (Viereck et al. 2016a, b) and allometric equations provided by Berner et al. (2015). The end product was a map in which age cohorts of each tree species, shrub species, and select moss functional types and their relative biomasses were defined for each cell. For additional documentation related to the construction of the initial map of vegetation communities, see appendices of Lucash et al. (2023).

A map of dead coarse root biomass was created using published relationships between dead coarse roots and live coarse roots (Yang et al. 2015) with

live root biomass data provided in the FIA-Tanana dataset (USDA-Forest Service 2018). A map of coarse woody debris was created using the downed wood table in the FIA-Tanana dataset and linking it to the corresponding imputed FIA plot for each cell.

Biophysical inputs

Maps of soil texture, soil depth, soil drainage class, field capacity, wilting point, and organic matter were created using the State Soil Geographic data available from USDA-NRCS for the state of Alaska at a 1:1,000,000 scale. Maximum relative gross primary productivity data across a range of soil water contents and soil temperature at 10 cm depth from Alaska Ameriflux sites (Iwahana 2019; Ueyama et al. 2023a, b, c) were used to fit nonlinear temperature and soil moisture response functions for four species functional groups: conifer, hardwood, shrubs, and mosses. Inputs to the SHAW module of DGS were sourced from a combination of literature values and GLUE analyses conducted by Marshall et al. (2021a, b). Inputs to the GIPL soil temperature module of DGS were obtained by assimilating temperature observations from sites across interior Alaska (Lucash et al. 2023).

Climate inputs

Daily weather inputs were needed to provide necessary climatological information for the succession and fire extensions of LANDIS-II. Climate data from two GCMs were used to create historical (1970-1999, NCAR-CCSM4 only) and RCP 8.5 future (2000–2100, GFDL-CM3 and NCAR-CCSM4) climate streams. The source dataset was downloaded from the Scenarios in Arctic Planning Group (SNAP) and was dynamically downscaled to 20 km resolution using the WRF model (Bieniek et al. 2016; Lader et al. 2017). Relative to other CMIP5 GCMs, NCAR-CCSM4 and GFDL-CM3 GCMs exhibit patterns that are close to the average and the high end of both temperature and precipitation out of available CMIP5 models, respectively (Marshall et al. 2021b; Fig. 1). While finer-scale downscaled climate data and additional climate scenarios are available for Alaska, those data sources did not include all required variables at a daily temporal resolution necessary to run



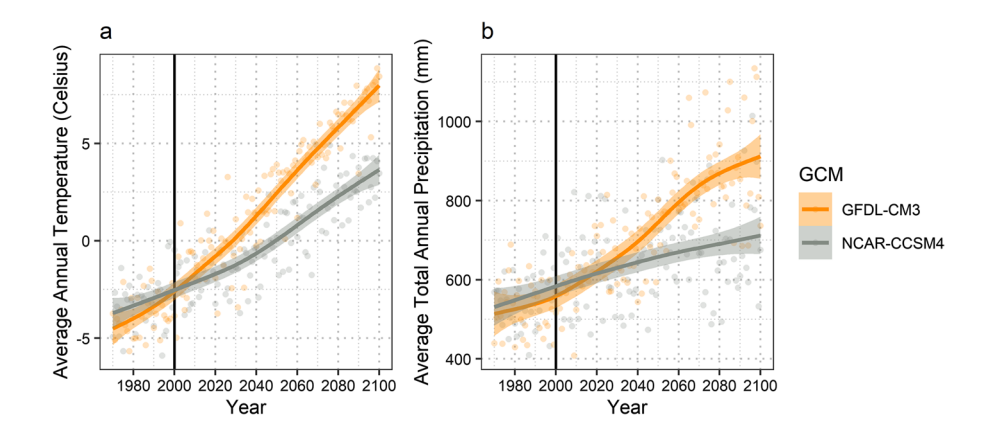


Fig. 1 Average annual temperature (a) and total precipitation (b) from climate inputs, averaged by area across all climate regions within the study landscape from two GCMs used in simulations. The vertical line indicates the division between

historical scenario data (1970–1999) and future scenario data (2000–2100). Generalized additive models of trends are also plotted with standard error

the SCRPPLE fire extension in LANDIS-II at the time when simulations were initiated.

LANDIS-II uses 'climate regions', which group areas on the landscape with similar climates and provide the same climate stream to all cells within a given region. Following the methodology of Lucash et al. (2019) a series of k-means cluster analysis of monthly climate data normals was done to identify areas of similar climate using the package 'cluster' in R (Maechler et al. 2021). Average monthly projected precipitation and temperature data from 2000 to 2100 were used as inputs and the analyses were done using the package 'cluster' in R (Maechler et al. 2021). We evaluated the optimal number of clusters by running 28 individual cluster analyses with the number of cluster solutions ranging from three to 30 and evaluating the resulting average silhouette values and sum of squares errors for the resulting cluster solutions (both measures of goodness-of-fit), based on pairwise distances between observations. A five-cluster solution was found to best maximize the average silhouette value (higher values indicate dense, well-separated clusters) while minimizing the sum of squares errors, so was determined optimal. Winter air temperature inversions often form in valley bottoms in interior Alaska (Malingowski et al. 2014), making these areas favorable for permafrost formation and preservation (Jorgenson et al. 2010). To capture this phenomenon within the model and represent greater climatic variation due to winter temperature inversions within each of the five initial climate regions, we ran additional cluster analyses within each region using mean winter air temperature from 30-year gridded normals (PRISM Climate Group: Oregon State University 2021), grouping each region into two subregions such that there would be a warm and cool region for each that would generally be associated with valleys and slopes across the landscape. Altogether, this process resulted in a total of ten climate regions.

The climate data had not been bias-corrected to ensure that the climate outputs were consistent with historical observations; therefore, we used a quantile mapping approach using the 'qmap' package in R (Gudmundsson and Gudmundsson 2012) with ERA-Interim reanalysis data (downscaled and provided by the same SNAP data source) to bias correct each variable for each climate region on the landscape. Values were extracted from each climate region for all climate variables at the center of the grid cell residing closest to each region's k-means cluster center (i.e., the grid cells most representative of each climate region). Precipitation was further adjusted to limit the effect of spatial aggregation that was present within the original data (including the ERA-Interim reanalysis data), which created days where there were exceptionally small amounts of precipitation and very few days without precipitation. On days where precipitation fell below one mm, precipitation was set to zero; the aggregate precipitation lost due to this correction was proportionally redistributed across days where precipitation fell above 1 mm.



Calibration of DGS model extension

The performance of DGS was calibrated and tested using field data specific to three sites representing different vegetation and successional states (a burned site, a black spruce-dominated site, and a deciduous site) and running single-cell simulations as representations of each site.

The individual growth of each species was calibrated by running single-cell simulations populated with single young (cohort age of one year with 100 gm⁻² biomass) cohorts for 200 years under historic climate forcing. Biomass trends from each single cell simulation were compared with FIA tree biomass data plotted against stand age as a proxy for the reference growth trajectory. Simulations were repeated with a set of varying parameters, selected based on there being greater uncertainty around their values (Appendix Table 4), which were adjusted iteratively within acceptable ranges using a particle swarm optimization algorithm approach with the hydroPSO package in R (Zambrano-Bigiarini and Rojas 2018) to find a solution where species single cohort trajectories bestmatched tree reference data (Appendix B).

To validate that simulated biomass trajectories following reburns were consistent with field data, a 20,000-ha test landscape was populated using field reference data of woody plant composition from plots measured at sites 12–15 years post-fire. Simulations of 200 years were run under historic climate forcing with wildfires. Trends in species biomass from cells that experienced a fire history consistent with reference plots from two sites (one categorized as upland and one as lowland) were compared (Fig. 4).

Description and parameterization of SCRPPLE extension

Wildfire was modeled dynamically using the SCRP-PLE fire extension (v. 3.2; Scheller et al. 2019). This extension allows for fire behavior to respond to climatic variables (e.g., fire weather index, wind velocity) and changes in fuel loading throughout the simulation period. Fire ignition probability is based on a Poisson model (Zuur et al. 2009) of historic daily ignitions and fire weather index (FWI), fit using records of regional historic ignitions (Short 2023; Appendix C) and corresponding daily fire weather derived from meteorological (met) station data (Menne et al. 2012).

Fire spreads from cell-to-cell based on a probability (logistic) function of daily fire spread, which calculates spread success based on the FWI, effective wind speed, and fine fuels (Scheller et al. 2019; Appendix C) until the maximum daily spread area is reached (Scheller et al. 2019). Maximum daily spread area was calculated based on a generalized linear model of historic daily fire areas versus FWI and effective wind speed (Appendix C). Parameters of daily spread were fit using historic daily fire perimeter data (GeoMAC 2019, 2020), met station data (Menne et al. 2012), topographic data (USGS 2020a), and fine fuels data (USGS 2020b).

The mortality from fires is driven by two functions: one determining site-level mortality and one cohort-level mortality. Site-level mortality is determined by an inverse link function of the percentage of clay in the soil, evapotranspiration in the year prior, effective wind speed during the fire, climatic water deficit the year prior, and fine fuels present during the fire. Cohort-level mortality is then determined by a combination of the site-level severity value, cohort age, and individual species' bark thickness. More information on the SCRPPLE fire extension v. 3.2 may be found on GitHub (https://github.com/LAN-DIS-II-Foundation/Extension-SCRPPLE).

Simulations

A total of 30 simulations were run; 10 were replicates of the historic climate data stream (using NCAR-CCSM4 historical data from SNAP), which served as the reference historic climate forcing scenario in the analysis. Ten replicates each of NCAR-CCSM4 (hereafter 'NCAR') and GFDL-CM3 (hereafter 'GFDL') RCP 8.5 scenarios were run to represent potential future conditions. Here, GFDL is interpreted as the more extreme (highest temperature and precipitation values by end of the century) of the two future scenarios (Fig. 1). Simulations were run for 100 years, with historic scenarios randomly sampling one year of data from the 30 available years in the stream annually, making sequences of climate inputs for each historic replicate unique. While each replicate was run with identical input parameters within each scenario, stochastic processes (e.g., wildfire, seed dispersal) resulted in non-identical end-of-century outcomes. Averages and variability were calculated across replicates in subsequent analyses to provide an estimate



of the variation in model outcomes as a result of these stochastic processes. All simulations were run on the CyVerse computing cluster (cyverse.org).

Analysis

Average landscape biomasses for each species were summarized over time to examine broad, landscapelevel trends for each scenario type across replicates. To analyze which cells changed vegetation state from a conifer-dominant condition and the site-specific variables associated with those cells, annual maps of species biomass from the Output Biomass extension (Scheller and Mladenoff 2004) were generated and used to determine vegetation type within each cell at each time step. This was then used to calculate the proportions of cells which transitioned away from conifer-dominance within each dataset to an alternative dominant vegetation type (e.g., deciduous, mixed broadleaf deciduous-conifer, or non-forest). Four vegetation types were used in the analysis based on relative tree species dominance: conifer dominant, mixed broadleaf deciduous-conifer dominant, broadleaf deciduous dominant, and non-forest. Cells were classified as broadleaf deciduous dominant if the percentage of total tree biomasses of paper birch (Betula neoalaskana), quaking aspen (Populus tremuloides), and balsam poplar (Populus balsamifera) together exceeded 66.66%; mixed conifer-broadleaf deciduous if the percentage of those same species out of the total were in between 33.33 and 66.66%, and conifer dominant if broadleaf tree species percentage was less than 33.33%. If tree biomass for a given cell was equal to zero, that cell was classified as non-forest..

Random Forests were trained to classify whether cells on the landscape would change to a vegetation state different from conifer dominant within the 10 years following the most recent wildfire and to assess the relative importance of potential drivers. The Random Forest algorithm can handle high-order interactions well, can be reliably used when predictors are highly correlated, and predictors can be a combination of categorical and continuous as is the case for this study (Strobl et al. 2008). The 10-year post-fire benchmark was selected because tree species within boreal forest communities that establish dominance within the first decade following a fire are likely to retain dominance until subsequent disturbances are experienced (Johnstone and Chapin

2006a; Johnstone et al. 2020). Predictors included a combination of continuous and categorical variables related to climate, climate variability, mortality from fire, starting species composition, topography, and neighborhood effects (Table 1).

Grid-cells classified as conifer-dominant at the start of the simulation were isolated and their fire histories (the number of fires experienced) were identified using output maps of wildfires that are produced at each timestep by the SCRPPLE extension. Of the cells that began the simulations as mature conifer, ten percent (n=1912) were then randomly sampled each from three fire categories: once burned, twice burned, or three times burned (evaluated up until the 90th year). This stratification was done to ensure a more balanced sampling from each fire category. Input datasets of predictors were then constructed by extracting associated values for variables of interest from sampled cells. Three random forest analysesone for each fire history type (one, two, and three wildfires) were run for each replicate set for a total of 30 random forests. Forests of 500 trees were trained for each with five variables sampled as candidates at each split. Forests were trained on 80% (n = 1,529) of each random forest dataset and prediction accuracy was determined using the remaining 20% (n=383). Conditional variable importance (Strobl et al. 2008) was extracted for each variable from the random forests and distributions of those values were plotted for comparison. Conditional variable importance gives higher values to those variables that are most important in successfully classifying the variable of interest (here, the transition from or retention of conifer dominance), while accounting for shared contributed importance (i.e., collinearity) among variables, thus ranking higher those variables that offer unique information beyond that which is shared. Lastly, additional exploratory analyses were conducted on variables that were identified as most important for each fire history model classifier to better understand the direction of those variables concerning post-fire retention or transition of conifer dominance. We used the R packages 'party' and 'permimp' to run and evaluate the Random Forests.



Table 1 Predictor variables included in Random Forest models predicting transitions from a conifer-dominated state to alternative states 10 years following one, two, and three fires in interior Alaska

Variable type	Specific variables	Categorical or continuous Initial data source	Initial data source
Climate - Scenario	Scenario (Historical vs. Future), general circulation model (NCAR-CCSM4 or GFDL-CM3), specific scenario (Historical, Future-NCAR or Future-GFDL)	Categorical	SNAP historical and projected dynamically downscaled climate data for the state of Alaska, 20 km resolution (Bieniek et al. 2016)
Climate - Temperature	Change in mean annual temperature between first and last five years of the simulation, mean and variance in annual temperature all years, mean and variance in annual temperature post-fire*	Continuous	SNAP historical and projected dynamically downscaled climate data for the state of Alaska, 20 km resolution (Bieniek et al. 2016)
Climate - Precipitation	Change in total annual precipitation between first and last five years of the simulation, mean and variance in total annual precipitation all years, total annual precipitation and variance in total annual precipitation post-fire*	Continuous	SNAP historical and projected dynamically downscaled climate data for the state of Alaska, 20 km resolution (Bieniek et al. 2016)
Fire effect	Percent total carbon removed, percent biomass removed (i.e., vegetation killed)	Continuous	Derived from model outputs. Calibrated from fire perimeter (GeoMAC 2019, 2020) and ignitions datasets for Alaska (Short 2023)
Fire effect	Fire year	Categorical	Derived from model outputs. Calibrated from fire perimeter (GeoMAC 2019, 2020) and ignitions datasets for Alaska (Short 2023)
Seed availability	Presence of adjacent (bordering) mature black spruce cells	Binary categorical	Derived from model output. Initial spatial distribution of the biomass density and ages of black spruce developed using forest inventory (USDA-Forest Service 2018) and landcover datasets (Alaska Center for Conservation Science 2017)
Seed availability	Number of adjacent (bordering) mature black spruce cells	Continuous	Derived from model output. Initial spatial distribution of the biomass density and ages of black spruce developed using forest inventory (USDA-Forest Service 2018) and landcover datasets (Alaska Center for Conservation Science 2017)
Soil/Hydrology - Soil temperature	Time 1 soil temperature at 3 m, mean and variance in soil temperature at 3 m post-fire*	Continuous	Calculated for specific temperature-hydrology units within DGS (see Lucash et al. 2023)
Soil/Hydrology - Soil moisture	Time 1 soil moisture at 0.55 m, mean and variance in soil moisture at 0.55 m post-fire*	Continuous	Calculated for specific temperature-hydrology units within DGS (see Lucash et al. 2023)
Starting species composition	Time 1 starting deciduous fraction	Continuous	Initial spatial distribution of the biomass density and ages of species were developed using FIA Tanana datasets (USDA-Forest Service 2018) and (Alaska Center for Conservation Science 2017)
Topography/landscape position	Aspect	Continuous	Derived from a digital elevation model for Alaska (USGS 2020a)



Table 1 (continued)			
Variable type	Specific variables	Categorical or continuous Initial data source	Initial data source
Topography/landscape position	Lowland vs upland status	Binary categorical	Derived from a digital elevation model for Alaska (USGS 2020a)

*Post-fire values are averages for the first decade post-fire

Results

Validation of successional trends

Simulated post-fire biomasses of broadleaf trees, coniferous trees, and shrubs matched field data within one standard deviation for all woody species groups except shrubs at the lowland sites after two and three fires, where biomasses were elevated and more variable than plot data (Fig. 2). Simulations yielded more variable post-fire biomasses in most cases, although they were the least variable for lowland broadleaf trees post-fire. In general, simulated tree biomasses were the most variable following one fire relative to subsequent fire events.

Landscape trends

The greatest increases in landscape biomass over the course of the simulation occurred under future climate change scenarios, primarily driven by increases in willow and alder (Alnus spp.) biomass, which increased more than 43-fold and 26-fold, respectively, between the start and end of the simulation (Fig. 3). However, tree biomass for all overstory tree species except for tamarack experienced declines of 45% (black spruce) up to 69% (paper birch). Vegetation type extents also changed over time across scenarios (Fig. 4); the conifer dominant vegetation type accounted for 63.1% (SD=1.9%) of the landscape by the end of the century when historical climate was used, an increase from the 56.5% present at the start of the simulation. Under future climate change scenarios, the conifer vegetation type was reduced to 54.3% (SD=2.6%, NCAR) and 44.7% (SD=3.1%, GFDL), whereas the deciduous-dominant vegetation type increased under climate change scenarios from 17.4% at the simulation start to 21.8% (SD=2.0%, NCAR) and 32.8% (SD = 2.7%, GFDL).

Changes in forest type occurred most often in cells on the landscape that experienced wildfire; cells that did not experience any wildfire generally remained the same vegetation type, regardless of the climate scenario used (Fig. 5a). In cells that experienced fire(s), shifts away from conifer dominance were most common when there was wildfire and under climate change and the frequency of these type shifts were most dramatic when more than one fire took place (Fig. 5c). Under climate change, the vegetation type



Fig. 2 Biomass densities of different functional groups in upland vs. lowland locations in interior Alaska compared to test simulations designed to mirror field site conditions and fire histories. Test simulations were initiated with data from unburned reference plots (Number of Fires = 0) and burned grid cells analyzed had experienced the most recent fire 12–15 years ago

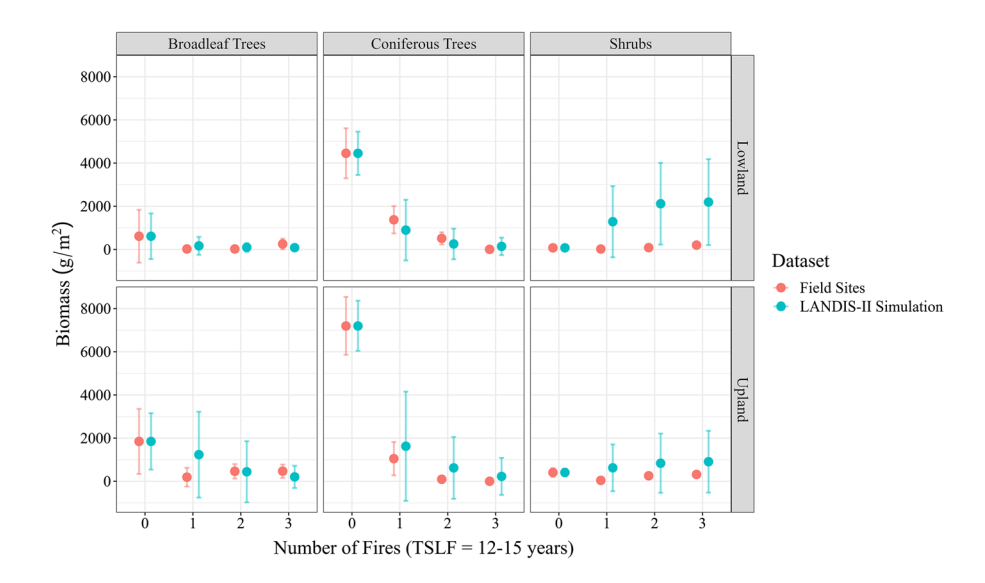
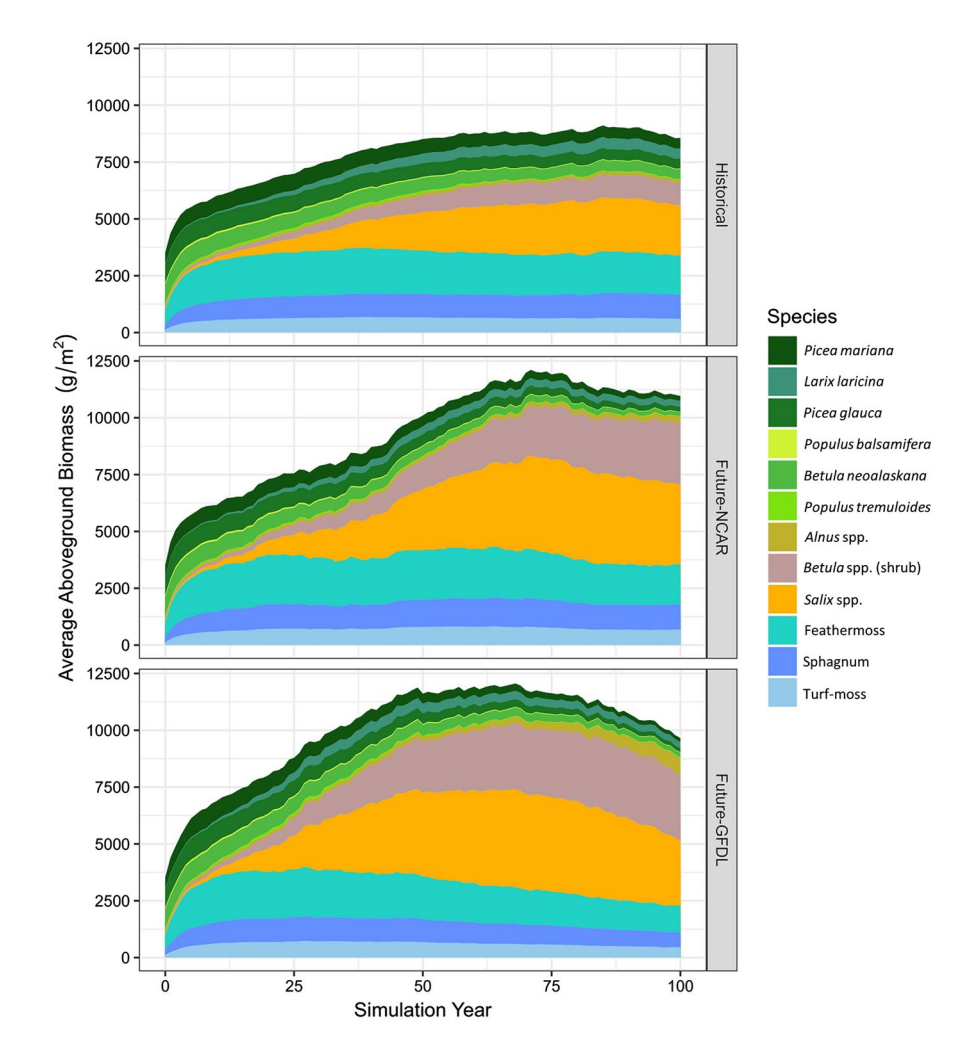


Fig. 3 Trends in biomass (gm⁻²) for each species simulated in one of three scenarios which include one historical scenario (using NCAR-CCSM4) and two future (both RCP 8.5, one using NCAR-CCSM4 and on using GFDL-CM3) averaged across ten replicates per scenario over time





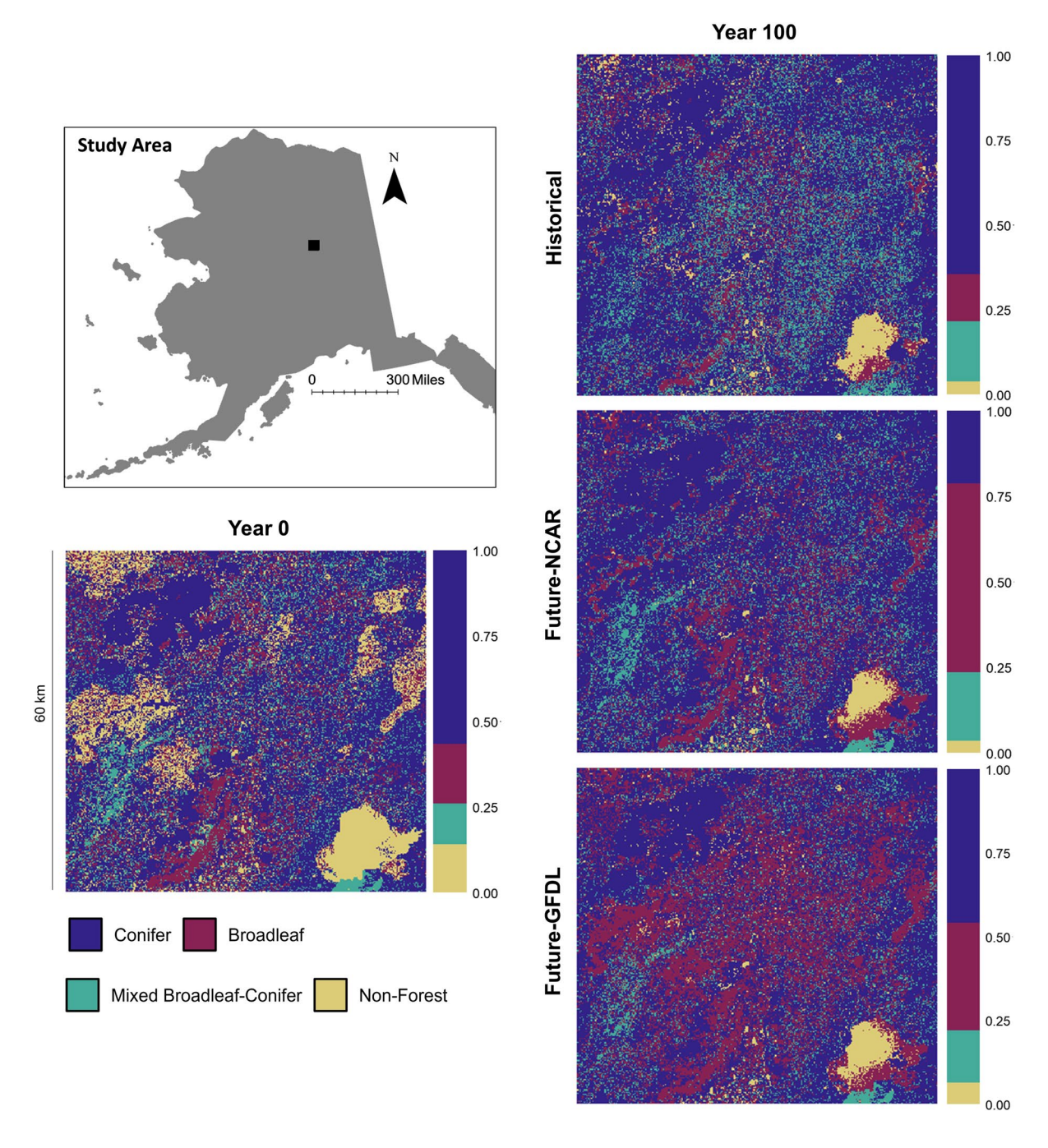


Fig. 4 Maps and stacked bar graphs showing the proportion of dominant overstory species at year 0 (left) and year 100 (right) for three climate scenarios for one example replicate. Study

area boundary within interior Alaska is displayed by the black square in the map at the upper left

which increased the most in extent on the landscape by the end of the century was the broadleaf group, with the most frequent shifts to this type occurring under the GFDL climate change scenario.

Burned cell trends

Across all scenarios, conifer dominance decreased in extent with the number of fires, while the number of



Fig. 5 a-c Proportions of total cells across ten replicate simulations within each dominant vegetation type for each scenario at years 0, 50, and 100, with pathways taken to the next consecutive vegetation type noted for cells that experienced zero (a), one (b) and three (c) fires throughout the simulation period

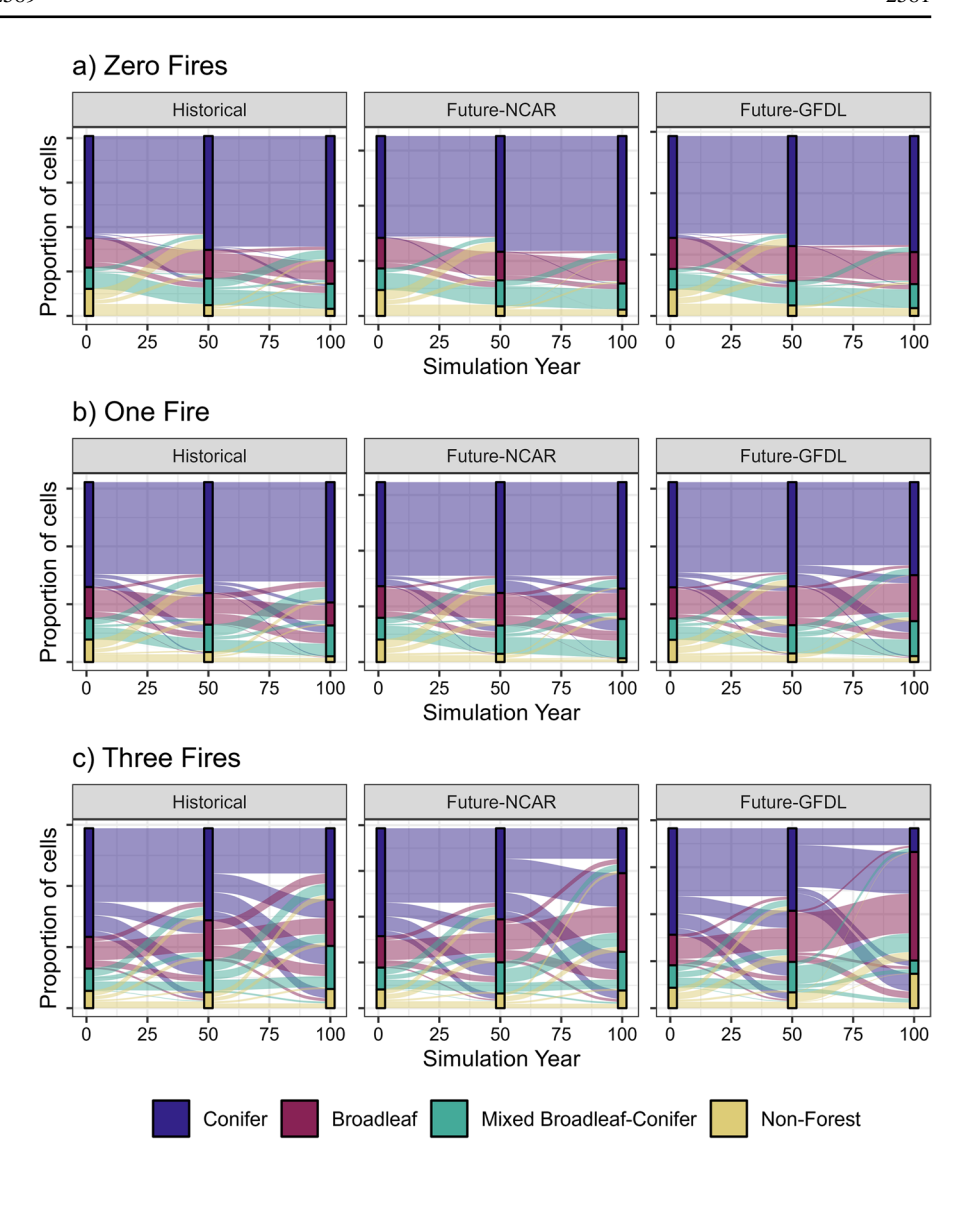
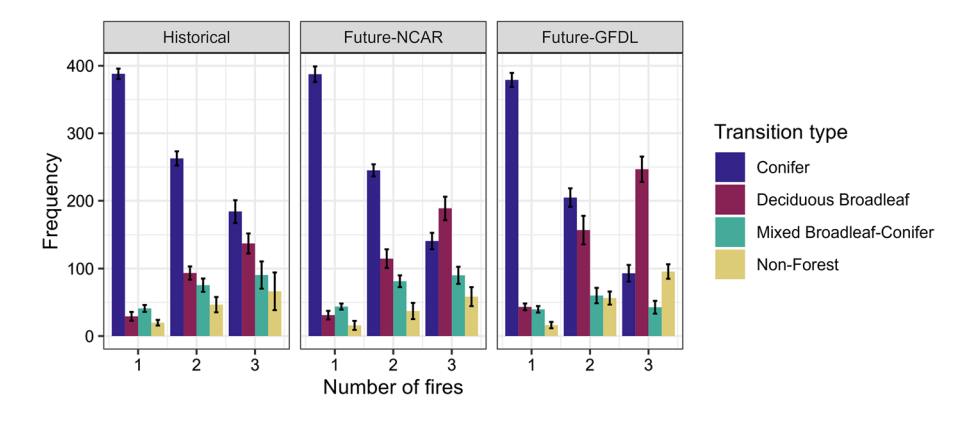


Fig. 6 Average frequency (±SD) of sampled grid cells within each vegetation type ten years following the most recent fire by the number of fires and scenario. All cells graphed here began the simulation as conifer vegetation type





cells that converted to an alternative vegetation type increased (Fig. 6). Conversion rates from conifer dominant to a mixed broadleaf deciduous-conifer vegetation type remained relatively constant between two and three fires after increasing between one and two fires (Fig. 6). The number of cells that converted to broadleaf vegetation types was greater for the future climate change scenarios. When three fires occurred under the future climate change scenarios, the number of grid cells that had converted to a broadleaf vegetation type were greater than those that retained conifer dominance.

The random forest models were able to classify conifer retention vs. transition at the cell scale with good accuracy on the independent test sets, performing best on the one-time fires and least well on the three-time fires $(1 \times accuracy = 85.7\%, SD = 1.6\%;$ $2 \times \text{accuracy} = 77.0\%$, SD = 2.0%; $3 \times \text{accuracy} = 76\%$, SD = 2%). Using random forest classification models for each fire history type, similar variables played an important role in predicting conifer retention vs. transition for once burned, twice burned, and thrice burned analyses. However, there were differences in the relative conditional importance between explanatory variables. Across all random forest analyses, the variable with the highest conditional importance for predicting the vegetation state of a cell ten years postfire was percent biomass loss (i.e., vegetation mortality) during the fire (Table 2). This variable was most important across all random forest models. Additional variables that were important in predicting post-fire vegetation state included starting deciduous fraction, percent of total carbon removed, both above and belowground carbon (post-pre-fire), and the number of adjacent cells containing mature conifer biomass. For a full list of variables and their corresponding conditional permutation importance values, see Appendix D.

Cells that did not maintain conifer-dominance post-fire tended to experience higher percentages of aboveground biomass loss from fire than those where conifer-dominance was retained. However, this difference in biomass loss was most distinct for single fire cells (Appendix E). The percent aboveground biomass removed also interacted with the number of surrounding cells with conifer biomass across the range of fires experienced. Two and three fire cells that retained conifer dominance tended to have greater numbers of surrounding mature conifer cells (i.e., potential seed sources) when they had lost a greater percentage of biomass (Appendix E).

For single fires, a lower starting deciduous fraction (at Time 1 of the simulation) was more associated with conifer retention—however, this effect was reduced for multiple fires (Appendix E). For reburns, state transitions happened more when the starting deciduous fraction was lower, especially in thrice burned cells that transitioned to non-forest. The percentage of total carbon removed was also an important predictor across the number of fires experienced. For single fire cells, cells that transitioned to non-forest had higher levels of carbon removal while cells that experienced multiple fires in general had lower percentages of carbon removed (Appendix E).

Discussion

There is growing concern that continuing trends in warming and increasing fire activity will lead to significant declines in conifer-dominance within the Alaskan boreal forest. When simulating a combination of both these processes (climate change and fire),

Table 2 The top five variables ranked by conditional permutation importance values out of 27 total input variables used in the random forest classification models of vegetation transition ten years following one (a), two (b), and three (c) fires

Rank	One fire	Two fires	Three fires
1	Percent biomass removed	Percent biomass removed	Percent biomass removed
2	Starting deciduous fraction	Percent total carbon removed	Starting deciduous fraction
3	Aspect	Number of adjacent black spruce cells	Number of adjacent black spruce cells
4	Upland vs. lowland	Starting deciduous fraction	Percent total carbon removed
5	Percent total carbon removed	Post-fire variance in precipitation	Post-fire variance in soil temperature at 3 m



we found that conifer forest extent did in fact decline, and the greatest decline occurred when there were multiple fires under the most extreme climate change scenario. Most frequently, conifer forest transitioned to a broadleaf deciduous vegetation type by the end of the simulation. These findings are consistent with field studies that have examined the effects of multiple and/or short-interval fires and have consistently found that when fires have burned with greater frequency (Hayes and Buma 2021), severity (Johnstone et al. 2010b, 2020; Mack et al. 2021) and with shorter than typical intervals (Johnstone and Chapin 2006a; Viglas et al. 2013; Whitman et al. 2019), transitions away from a conifer-dominant state occurred. These transitions have been tied to a decline in seed availability (Viglas et al. 2013) and changes in the post-fire depth of the soil organic layer (Johnstone et al. 2010b, 2020; Hayes and Buma 2021), as well as interactions with climate (e.g., drought; Whitman et al. 2019; Walker et al. 2017).

We also found that drivers of conifer forest transitions were similar regardless of the number of fires experienced during the simulation period, and most important was the percentage of aboveground biomass killed during the most recent fire, a dimension of fire severity. Fire severity in field studies is often defined using composite burn indices in remote sensing work or by measuring consumption of soil organic layer in field studies (Boby et al. 2010). Past field studies have found that higher severity wildfire promotes the recruitment of broadleaf deciduous species post-fire (Shenoy et al. 2011; Hollingsworth et al. 2013; Mack et al. 2008), reflecting the importance of residual aboveground biomass post-fire in shaping relative overstory dominance. Across simulations, the percent vegetation mortality from wildfire was high (mean = 80.3%, SD = 27.3%), which is characteristic of black spruce ecosystems (Boby et al. 2010; Hollingsworth et al. 2013). Variation within those high levels of mortality appears to have strong predictive power of post-fire vegetation trajectories. This is consistent with the findings of Hollingsworth et al. (2013) who found that post-fire community composition was primarily related to severity gradients, as measured via combustion of biomass and residual vegetation.

Beyond vegetation consumption, total carbon removed by wildfire, including the belowground carbon pool, was also an important conditional predictor of post-fire black spruce retention in twice burned and thrice burned random forest models. The DGS extension does not capture the effect of soil organic matter depth on seedling establishment (via exposed mineral soil), which could have contributed to the relatively lower importance of this variable compared with biomass loss and this is an area of potential future model development work. However, other belowground competition dynamics are captured within DGS; species with adventitious roots have access to water near the soil surface within the model, while other species do not, giving black spruce an advantage over its deciduous counterparts which lack this adaptation, especially when permafrost is present and water availability is restricted to near surface depths (Lebarron 1945; Krause and Lemay 2022). The importance of total carbon loss could indicate other effects of belowground organic matter consumption, such as soil temperature and subsequent permafrost freeze/thaw dynamics. Reduction in soil organic matter post-fire contributes to permafrost degradation and increases soil microbial activity, releasing nutrients and moisture and providing an advantage to species with greater rooting depths and nutrient needs that would otherwise be restricted by permafrost and a shallow active layer (e.g., broadleaf deciduous species; Sturm et al. 2005). Within DGS, vegetation type, associated soil characteristics, and landscape position influence belowground thermal dynamics. Rooting depths are specified for each species and the ability of a cohort to access water and nutrients is limited to unfrozen soil layers, such that those species with deeper rooting depths gain an advantage on sites with near-surface permafrost degradation. These belowground thermal dynamics may have encouraged deciduous vegetation transitions when fire severity was high and promoted greater permafrost thaw depths.

Other important factors for predicting conifer retention or transition were cell adjacency of mature black spruce in the most recent fire year and starting proportion of broadleaf deciduous biomass. When additional fires were experienced (reburns), factors beyond biomass removal alone became more important in determining whether self-replacement of the conifer vegetation type. Black spruce has a relatively short seeding distance (typically within 80 m; Johnston 1971; Tuskan and Laughlin 1991), not exceeding the Euclidean distance of one 4-ha cell (200–283 m), constraining seed dispersal to just those cells which



are adjacent to a given site. This relatively short seeding distance makes the species vulnerable to seed source limitation and immaturity risk should existing nearby seed sources become less available or remain below the age of sexual maturity (Johnstone and Chapin 2006a; Viglas et al. 2013). Results show that cells with potential seed sources as neighbors (adjacent mature conifer cells) are buffered against the effect of higher biomass loss events more than their counterparts with fewer adjacent seed sources. Additionally, when broadleaf deciduous species have lower relative biomass at the start of the simulation, this increases conifer retention post-fire. This result is consistent with field studies, which have found that high densities of pre-fire black spruce are advantageous for post-fire reestablishment (Johnstone and Chapin 2006a; Johnstone et al. 2010a).

Under climate change, transitions to a broadleaf deciduous forest type were observed at greater rates following wildfire than a mixed-deciduous forest type, which includes levels of conifer biomass and broadleaf biomass both within 33-66% of total tree biomass. This indicates that under combined pressures of multiple fires and/or climate change, when coniferdominated forests transition to an alternate state, it does so by swiftly transitioning into a broadleaf-dominated forest, rather than gradually shifting species' relative dominance over time. This type of abrupt transition is characteristic of nonlinear behavior and a system approaching an ecological tipping point (Scheffer and Carpenter 2003; Lenton 2012). Tipping points imply that there are positive feedbacks internal to the system promoting self-amplification of a given state (Lenton 2012). In interior Alaska, past work has supported the existence of these internal feedbacks promoting either conifer or broadleaf dominance as each given state creates and perpetuates specific soil temperature, nutrient, and microbial feedbacks (Chapin et al. 2004; Kurkowski et al. 2008; Johnstone et al. 2016). Under the singular pressure of greater numbers of fires (which necessitates a lower mean fire return interval in these 100-year simulations) under historic climate, transition rates to broadleaf forest type nearly doubled after two fires (increased by 84%) and increased an additional 24% after three fires. With climate change, those rates of transition to broadleaf deciduous dominance increased even more aggressively and outpaced conifer retention rates after three fires in the Future-GFDL climate scenario. This combination of climate pressure and multiple fires may represent a threshold whereupon the broadleaf forest type transitions become more common.

These findings are consistent with other process modeling work from interior Alaska that have projected state shifts from conifer to broadleaf deciduous dominance at large scales with the interaction of climate change pressure and wildfire activity driving forest type change (Mann et al. 2012; Foster et al. 2019; Mekonnen et al. 2019; Hansen et al. 2021). Mekonnen et al. (2019) and Foster et al. (2019) included below-ground dynamics in their simulations and found climate-induced changes on these processes were a key mechanism for reinforcing changes in vegetation composition. Similarly, in this study climate change was an exacerbating factor in accelerating transitions to the alternate broadleaf forest state, potentially due to increases in soil temperatures that both increased thaw depths (i.e., increasing the potential rooting zone) and accelerated nitrogen mineralization. Hansen et al. (2021) tested the stability of a newly transitioned deciduous state in their simulation study, and found that the broadleaf deciduous forest state was highly resilient once established. This further supports the idea of there being a critical threshold between conifer and deciduous dominated states, with mixed-conifer forest types being a relatively less common transition, as we observed in our simulations.

The increase in biomass over time observed in this study was largely driven by the landscape-wide increase in shrub biomass. Studies from other high latitude systems have documented woody species expansion into tundra landscapes under climate change. Winter warming in the tundra has been correlated with increases in shrub abundance and greening patterns in boreal North America and Russia (Sturm et al. 2005; Bunn and Goetz 2006; Tape et al. 2006; Forbes et al. 2010). In tundra environments, shrub presence leads to warmer winter soil temperatures and greater soil microbial activity via interactions with snow depth, which in turn increases plant-available nitrogen in the soil and further promotes shrub growth in the subsequent growing season (Sturm et al. 2005; Myers-Smith et al. 2011). Warming soils and increasing permafrost thaw depths in our simulation within the boreal forest could also be promoting greater nitrogen availability and encouraging the observed shrub growth. However, the increase in



shrub biomass is simulated even under historic climate conditions and we did not also observe a similar increase in overstory broadleaf deciduous species biomass density. Parameter uncertainty in the simulated shrub species may be one contributing factor in these patterns; data from two locations in interior Alaska within the Amerflux network (US-Rpf and US-Fcr; Ueyama et al. 2023b, c) were used to parameterize the temperature response curves of the shrub functional type. Shrub temperature response curves which internally operate within DGS are informed by these field observations, which reflect and greater relative gross primary productivity at higher temperatures relative to overstory counterparts (Appendix F). While rooted in field observations, the number of sites available and used in parameterizing this functional group were limited and more targeted analyses of growth rates in shrubs within boreal forest contexts is warranted to confirm these results and better understand how shrub species may continue to respond to warming.

Shrub biomass accumulation elevated beyond our expectations could also indicate a process absent from the modeling experiment that would otherwise limit the large accumulation of the willow (Salix spp.) and dwarf birch (Betula nana/Betula glandulosa) biomass observed in all three scenarios. One candidate process is herbivory by moose (Alces alces) and snowshoe hare (Lepus americanus). Both are known to influence boreal shrub communities (Myers-Smith et al. 2011; Bryant et al. 2014; Christie et al. 2015), though the relative strength of their influence under climate change warrants greater study (Christie et al. 2015). One study evaluated shrub radial growth in northern interior Alaska to examine the effect of browse pressure on climate-driven enhanced shrub growth and found that the positive warming effect on shrubs was, in part, offset by browsing, though not entirely (Frank 2020). Without the inclusion of this process within the modeling framework, it is difficult to conclude what the potential effect and interaction of this additional disturbance would be, or how herbivores would be impacted by direct and indirect effects of climate, vegetation, and fire processes. However, it is possible that they would at least partially moderate the strong growth response observed in this functional group. Herbivory has been frequently neglected in boreal landscape-scale successional dynamics models, although there is growing interest to better understand its role. Hansen et al. (2021) modeled successional trajectories within boreal forests and included browsing intensity as a factor, finding that chronic browsing combined with long fire free periods could limit the dominance of broadleaf deciduous tree species over black spruce. Further model development work is needed to better represent and understand these dynamics between shrub growth, climate change, herbivory, and forest succession.

The scenarios modeled in this study were limited by the GCM data that was available for interior Alaska, with options being restricted to those that contained the necessary climate variables needed for model inputs. The daily temporal resolution required to run the SCRPPLE extension constrained options for downscaled GCM data sources. Climate inputs were also aggregated to climate regions, and this combination of coarse resolution and spatial aggregation may provide one explanation for the low importance of climate variables in the random forest classification; there may have been a mismatch between the scale at which climate influences operated on post-fire successional processes that were not able to be captured here. Despite this, notable differences in composition outcomes were observed between climate scenarios across cells experiencing the same number of fires (Fig. 6), indicating that climatic factors are still likely influencing post-reburn vegetation dynamics beyond or in combination with the influence of fire. Further work disentangling climatic drivers from other factors at finer scales is needed as additional climate projections and scenarios become available for this region.

Overall, we simulated increases in landscape biomass over time, contributed especially by shrub species, emphasizing a need to better understand the role of these less-studied and modeled species in interior Alaska boreal forest communities under a warming climate. Quantifying changes to belowground pools of carbon and how they compare to these projected increases in aboveground biomass was outside of the scope of this study, however, future work with this focus will be critical to understanding whether boreal forests in interior Alaska and elsewhere are likely to continue functioning as a global carbon sink. Transitions from a conifer-dominant state to deciduous dominance were found to accelerate under climate change and increasing pressure from repeat wildfires, with factors related to fire severity and vegetation community context (e.g., starting relative dominance



and seed source) being important to predicting these transitions. These findings illustrate the potential for wildfire and climate warming to expand the distribution of deciduous dominance, especially under the warmest and wettest climate scenario. This has profound consequences for plant and animal communities, as well as, the indigenous human populations that have lived for millennia in boreal ecosystems. Given their massive extent, these changes could also have substantial consequences for global water balance, wildfire, and albedo, and alter feedbacks to the climate system.

Acknowledgments This work was supported by the National Science Foundation Award 1737706, and by the University of Oregon Department of Geography Rippey Dissertation Writing Grant. We thank Dr. Robert Scheller and Dr. John McNabb for their work converting code from the Damm-MCNiP and SHAW models to C# so they could be coupled into the DGS modeling framework. We thank Dr. Zachary Robbins for his help and advice on parameterizing the SCRPPLE extension to LANDIS-II. We are also grateful to Dr. Lucas Silva, Dr. Daniel Gavin, and Dr. Joshua Roering for their review of an early version of this work and feedback on the study design and results. We also thank CyVerse for use of their cloud computing resources (NSF Award DBI-1743442) which we used to run simulations and to Dr. Tyson Swetnam for his help in containerizing LANDIS-II and integrating the model into the CyVerse Discovery Environment. Lastly, we recognize the Bonanza Creek LTER (NSF Award DEB-1636476), which provided field data used in the parameterization of the DGS model. We also appreciate the feedback from two anonymous reviewers, whose input improved the clarity and presentation of results from the study.

Author Contributions SW: primary author of the manuscript; contributed to study design; parameterized and calibrated the DGS and SCRPPLE extensions, and was the primary contributor to the analysis. AM: provided parameters for SHAW and evaluated model performance of the SHAW component of DGS. KH: provided field validation data and feedback on validating vegetation response to reburns within the simulated landscape. DN: provided parameters for GIPL and evaluated model performance of the GIPL component of DGS. BB: contributed to the original study proposal and design; provided field data and feedback on vegetation inputs and validation. ML: principal investigator on original study proposal; contributed to study design and led DGS model development; provided parameters for the Damm-MCNiP module and evaluated model performance. All authors contributed to editing the paper and approved the final manuscript.

Funding This work was supported by the National Science Foundation Award 1737706, and by the University of Oregon Department of Geography Rippey Dissertation Writing Grant.

Data availability The datasets used to develop model inputs are cited within the manuscript and are available in the public

domain. DGS model inputs for this study are available in the LANDIS-II-Foundation repository at: https://github.com/LAN-DIS-II-Foundation/Project-Alaska-Reburns.

Declarations

Competing Interests The authors declare no competing interests.

References

- Abramoff RZ, Davidson EA, Finzi AC (2017) A parsimonious modular approach to building a mechanistic belowground carbon and nitrogen model. J Geophys Res Biogeosci 122:2418–2434.
- Alaska Center for Conservation Science (2017) Alaska vegetation and wetland composite map. https://accscatalog.uaa. alaska.edu/dataset/alaska-vegetation-and-wetland-composite. Accessed 17 Jan 2022
- Begét JE, Stone D, Verbyla DL (2006) Regional overview of interior Alaska. Alaska's changing boreal forest. Oxford University Press, New York, pp 12–20
- Berner LT, Alexander HD, Loranty MM et al (2015) Biomass allometry for alder, dwarf birch, and willow in boreal forest and tundra ecosystems of far northeastern Siberia and north-central Alaska. For Ecol Manage 337:110–118.
- Bieniek PA, Bhatt US, Walsh JE et al (2016) Dynamical downscaling of ERA-interim temperature and precipitation for Alaska. J Appl Meteorol Climatol 55:635–654.
- Boby LA, Schuur EAG, Mack MC et al (2010) Quantifying fire severity, carbon, and nitrogen emissions in Alaska' s boreal forest. Ecol Appl 20:1633–1647
- Bryant JP, Joly K, Chapin FS et al (2014) Can antibrowsing defense regulate the spread of woody vegetation in arctic tundra? Ecography 37:204–211.
- Buma B, Brown CD, Donato DC et al (2013) The impacts of changing disturbance regimes on serotinous plant populations and communities. Bioscience 63:866–876
- Bunn AG, Goetz SJ (2006) Trends in satellite-observed circumpolar photosynthetic activity from 1982 to 2003: the influence of seasonality, cover type, and vegetation density. Earth Interact 10:1–19.
- Burns RM, Honkala BH (1990) Silvics of North America: 1.
 Conifers; 2. Hardwoods. Agriculture Handbook 654. US
 Department of Agriculture, Forest Service, Washington,
 DC
- Carmean WH, Hahn JT, Jacobs RD (1989) Site index curves for forest tree species in the eastern United States. General technical report NC-128. St Paul, MN: US Dept of Agriculture, Forest Service, North Central Forest Experiment Station. 142 p
- Chapin FS, Callaghan TV, Bergeron Y et al (2004) Global change and the boreal forest: thresholds, shifting states or gradual change? Ambio 33:361–365.
- Christie KS, Bryant JP, Gough L et al (2015) The role of vertebrate herbivores in regulating shrub expansion in the Arctic: a synthesis. Bioscience 65:1123–1133.



- Fisher JP, Estop-Aragonés C, Thierry A et al (2016) The influence of vegetation and soil characteristics on active-layer thickness of permafrost soils in boreal forest. Glob Chang Biol 22:3127–3140.
- Flannigan M, Stocks B, Turetsky M, Wotton M (2009) Impacts of climate change on fire activity and fire management in the circumboreal forest. Glob Chang Biol 15:549–560.
- Flerchinger GN (2000) The simultaneous heat and water (SHAW) model: technical documentation. Technical Report NWRC 2000-09. Boise, ID: USDA Agricultural Research Service, Northwest Watershed Research Center. 37 p. URL https://www.ars.usda.gov/ARSUserFiles/20520000/shawdocumentation.pdf
- Forbes BC, Fauria MM, Zetterberg P (2010) Russian Arctic warming and "greening" are closely tracked by tundra shrub willows. Glob Chang Biol 16:1542–1554.
- Foster AC, Armstrong AH, Shuman JK et al (2019) Importance of tree- and species-level interactions with wild-fire, climate, and soils in interior Alaska: implications for forest change under a warming climate. Ecol Modell 409:108765.
- FRAMES (2023) Alaska Large Fire Database. URL https://www.frames.gov/catalog/10465. Accessed 2019
- Frank P (2020) Herbivory moderates the positive effect of climate warming on shrub growth in Northern Interior Alaska [Unpublished master's thesis]. Norwegian University of Science and Technology, Trondheim, Norway
- GeoMAC (2019) Historic perimeters combined 2000–2018. U.S. geological survey. Accessed 14 Aug 2020
- GeoMAC (2020) Historic Perimeters 2019, U.S. geological survey. https://data-nifc.opendata.arcgis.com/datasets/ nifc::historic-perimeters-2019/about. Accessed 14 Aug 2020
- Greene DF, Macdonald SE, Haeussler S et al (2007) The reduction of organic-layer depth by wildfire in the North American boreal forest and its effect on tree recruitment by seed. Can J For Res 37:1012–1023.
- Gudmundsson L, Gudmundsson ML (2012) Package 'qmap.' Methods 2012:3383–3390
- Hansen WD, Fitzsimmons R, Olnes J, Williams AP (2021) An alternate vegetation type proves resilient and persists for decades following forest conversion in the North American boreal biome. J Ecol 109:85–98.
- Hayes K, Buma B (2021) Effects of short-interval disturbances continue to accumulate, overwhelming variability in local resilience. Ecosphere. https://doi.org/10.1002/ecs2.3379
- Higuera PE, Brubaker LB, Anderson PM et al (2009) Vegetation mediated the impacts of postglacial climate change on fire regimes in the south-central Brooks Range, Alaska. Ecol Monogr 79:201–219.
- Hollingsworth TN, Johnstone JF, Bernhardt EL, Chapin FS (2013) Fire severity filters regeneration traits to shape community assembly in Alaska's boreal forest. PLoS ONE. https://doi.org/10.1371/journal.pone.0056033
- Hoy EE, Turetsky MR, Kasischke ES (2016) More frequent burning increases vulnerability of Alaskan boreal black spruce forests. Environ Res Lett 11:095001
- Iwahana G, Kobayashi H, Ikawa H, Suzuki R (2019) Ameri-Flux BASE US-Prr Poker Flat Research Range Black Spruce Forest, Ver. 3-5, AmeriFlux AMP, (Dataset). https://doi.org/10.17190/AMF/1246153

- Johnston WF (1971) Management guide for the black spruce type in the Lake States. Research paper NC-64. St. Paul, MN: US Department of Agriculture, Forest Service, North Central Forest Experiment Station
- Johnstone JF, Chapin FS (2006a) Fire interval effects on successional trajectory in boreal forests of northwest Canada. Ecosystems 9:268–277.
- Johnstone JF, Chapin FS (2006b) Effects of soil burn severity on post-fire tree recruitment in boreal forest. Ecosystems 9:14–31.
- Johnstone J, Boby L, Tissier E et al (2009) Postfire seed rain of black spruce, a semiserotinous conifer, in forests of interior Alaska. Can J For Res 39:1575–1588.
- Johnstone JF, Chapin FS, Hollingsworth TN et al (2010a) Fire, climate change, and forest resilience in interior Alaska. Can J For Res 40:1302–1312.
- Johnstone JF, Hollingsworth TN, Chapin FS, Mack MC (2010b) Changes in fire regime break the legacy lock on successional trajectories in Alaskan boreal forest. Glob Chang Biol 16:1281–1295.
- Johnstone JF, Allen CD, Franklin JF et al (2016) Changing disturbance regimes, ecological memory, and forest resilience. Front Ecol Environ 14:369–378.
- Johnstone JF, Celis G, Chapin FS et al (2020) Factors shaping alternate successional trajectories in burned black spruce forests of Alaska. Ecosphere. https://doi.org/10.1002/ecs2. 3129
- Jorgenson MT, Romanovsky V, Harden J et al (2010) Resilience and vulnerability of permafrost to climate change. Can J For Res 40:1219–1236
- Kasischke ES, Verbyla DL, Rupp TS et al (2010) Alaska's changing fire regime—implications for the vulnerability of its boreal forests. Can J For Res 40:1313–1324
- Krause C, Lemay A (2022) Root adaptations of black spruce growing in water-saturated soil. Can J For Res 52:653–661.
- Kurkowski TA, Mann DH, Rupp TS, Verbyla DL (2008) Relative importance of different secondary successional pathways in an Alaskan boreal forest. Can J For Res 38:1911–1923.
- Lader R, Walsh JE, Bhatt US, Bieniek PA (2017) Projections of twenty-first-century climate extremes for Alaska via dynamical downscaling and quantile mapping. J Appl Meteorol Climatol 56:2393–2409.
- Lebarron RK (1945) Adjustment of black spruce root systems to increasing depth of peat. Ecology 26:309–311
- Lenton TM (2012) Arctic climate tipping points. Ambio 41:10–22.
- Lucash MS, Ruckert KL, Nicholas RE et al (2019) Complex interactions among successional trajectories and climate govern spatial resilience after severe windstorms in central Wisconsin, USA. Landsc Ecol 34:2897–2915.
- Lucash MS, Marshall AM, Weiss SA, McNabb JW, Nicolsky DJ, Flerchinger GN, Link TE, Vogel JG, Scheller RM, Abramoff RZ, Romanovsky VE (2023) Burning trees in frozen soil: simulating fire, vegetation, soil, and hydrology in the boreal forests of Alaska. Ecol Model 481:110367
- Lynch JA, Clark JS, Bigelow NH et al (2002) Geographic and temporal variations in fire history in boreal ecosystems of Alaska. J Geophys Res 107:8152.



- Mack MC, Treseder KK, Manies KL et al (2008) Recovery of aboveground plant biomass and productivity after fire in mesic and dry black spruce forests of interior Alaska. Ecosystems 11:209–225.
- Mack MC, Walker XJ, Johnstone JF et al (2021) Carbon loss from boreal forest wildfires offset by increased dominance of deciduous trees. Science 372:280–283
- Maechler M, Rousseeuw P, Struyf A et al (2021) Cluster: cluster analysis basics and extensions. R Package Version 2(1):2
- Malingowski J, Atkinson D, Fochesatto J et al (2014) An observational study of radiation temperature inversions in Fairbanks, Alaska. Polar Sci 8:24–39.
- Mann D, Rupp T, Olson M, Duffy P (2012) Is Alaska's boreal forest now crossing a major ecological threshold? Arct Antarct Alp Res 44:319–331.
- Marchenko SS, Romanovsky VE, Tipenko G (2008) Numerical modeling of permafrost dynamics in Alaska using a high spatial resolution dataset. In: Proceedings of the ninth international conference on permafrost, pp. 1125–1130
- Marshall AM, Link TE, Flerchinger GN et al (2021a) Ecohydrological modelling in a deciduous boreal forest: model evaluation for application in non-stationary climates. Hydrol Process 35:1–18.
- Marshall AM, Link TE, Flerchinger GN, Lucash MS (2021b) Importance of parameter and climate data uncertainty for future changes in boreal hydrology. Water Resour Res 57:1–20.
- Mekonnen ZA, Riley WJ, Randerson JT et al (2019) Expansion of high-latitude deciduous forests driven by interactions between climate warming and fire. Nat Plants 5:952–958.
- Menne MJ, Durre I, Vose RS et al (2012) An overview of the global historical climatology network-daily database. J Atmos Ocean Technol 29:897–910.
- Myers-Smith IH, Forbes BC, Wilmking M et al (2011) Shrub expansion in tundra ecosystems: dynamics, impacts and research priorities. Environ Res Lett. https://doi.org/10. 1088/1748-9326/6/4/045509
- Nelson FE, Anisimov OA, Shiklomanov NI (2001) Subsidence risk from thawing permafrost. Nature 410:889–890.
- Nicolsky DJ, Romanovsky VE, Panda SK et al (2017) Applicability of the ecosystem type approach to model permafrost dynamics across the Alaska north slope. J Geophys Res Earth Surf 122:50–75.
- PRISM Climate Group: Oregon State University (2021) Recent 30 year normals (1981–2021). Oregon State University
- Rowland JC, Mancino A, Marsh P et al (2010) Arctic landscapes in transition: responses to thawing permafrost. Eos (Washington DC) 91:229–230
- Scheffer M, Carpenter SR (2003) Catastrophic regime shifts in ecosystems: linking theory to observation. Trends Ecol Evol 18:648–656.
- Scheller RM, Mladenoff DJ (2004) A forest growth and biomass module for a landscape simulation model, LAN-DIS: design, validation, and application. Ecol Model 180:211–229.
- Scheller RM, Domingo JB, Sturtevant BR et al (2007) Design, development, and application of LANDIS-II, a spatial landscape simulation model with flexible temporal and spatial resolution. Ecol Model 201:409–419.

- Scheller RM, Hua D, Bolstad Pv et al (2011) The effects of forest harvest intensity in combination with wind disturbance on carbon dynamics in Lake States mesic forests. Ecol Model 222:144–153.
- Scheller R, Kretchun A, Hawbaker TJ, Henne PD (2019) A landscape model of variable social-ecological fire regimes. Ecol Model 401:85–93.
- Shabaga JA, Bracho R, Klockow PA et al (2022) Shortened fire intervals stimulate carbon losses from heterotrophic respiration and reduce understorey plant productivity in boreal forests. Ecosystems. https://doi.org/10.1007/s10021-022-00761-w
- Shenoy A, Johnstone JF, Kasischke ES, Kielland K (2011) Persistent effects of fire severity on early successional forests in interior Alaska. For Ecol Manage 261:381–390.
- Short KC (2023) Spatial wildfire occurrence data for the United States, 1992–2018 [FPA_FOD_20210617]: 5th edition. Forest Service Research Data Archive. https://doi.org/10.2737/RDS-2013-0009.5. Accessed 2019
- Stralberg D, Arseneault D, Baltzer JL et al (2020) Climatechange refugia in boreal North America: what, where, and for how long? Front Ecol Environ 18:261–270.
- Strobl C, Boulesteix AL, Kneib T et al (2008) Conditional variable importance for random forests. BMC Bioinf 9:1–11.
- Sturm M, Schimel J, Michaelson G et al (2005) Winter biological processes could help convert arctic tundra to shrubland. Bioscience 55:17–26.
- Tape K, Sturm M, Racine C (2006) The evidence for shrub expansion in northern Alaska and the Pan-Arctic. Glob Chang Biol 12:686–702.
- Taylor PC, Cai M, Hu A et al (2013) A decomposition of feed-back contributions to polar warming amplification. J Clim 26:7023–7043.
- Tuskan GA, Laughlin K (1991) Windbreak species performance and management practices as reported by Montana and North Dakota landowners. J Soil Water Conserv 46:225–228
- Ueyama M, Iwata H, Harazono Y (2023a) AmeriFlux BASE US-Uaf University of Alaska, Fairbanks, Ver. 11-5, AmeriFlux AMP. https://doi.org/10.17190/AMF/1480322
- Ueyama M, Iwata H, Harazono Y (2023b) AmeriFlux BASE US-Fcr Cascaden Ridge Fire Scar, Ver. 3-5, AmeriFlux AMP. https://doi.org/10.17190/AMF/1562388
- Ueyama M, Iwata H, Harazono Y (2023c) AmeriFlux BASE US-Rpf Poker Flat Research Range: Succession from fire scar to deciduous forest, Ver. 9-5, AmeriFlux AMP. https://doi.org/10.17190/AMF/1579540
- USDA-Forest Service (2018) PNW-FIA interior Alaska database. https://www.fs.usda.gov/pnw/tools/pnw-fia-interioralaska-database.
- USGS (2020a) Alaska 2 Arc-second Digital Elevation Models (DEMs). https://data.usgs.gov/datacatalog/data/USGS: 4bd95204-7a29-4bd4-acce-00551ecaf47a
- USGS (2020b) LANDFIRE 2020b fuel characteristic classification system (FCCS) AK 2022 capable fuels. https://landfire.gov/metadata/lf2020b/AK/LA22_FCCS_220.
- Van Cleve K, Dyrness CT, Viereck LA et al (1983) Taiga in ecosystems interior Alaska. Bioscience 33:39–44
- Viereck LA, Van Cleve K, Chapin FS, Ruess RW, Hollingsworth TN, Bonanza Creek LTER (2016a) Vegetation



- Plots of the Bonanza Creek LTER Control Plots: Species Count (1975 2004) ver 20. Environmental Data Initiative. https://doi.org/10.6073/pasta/8dd0e1ac48e2f82b51adabfbd3c62ae2. Accessed 2020
- Viereck LA, Van Cleve K, Chapin FS, Hollingsworth RW (2016b) Vegetation plots of the Bonanza Creek LTER control plots: species percent cover (1975–2009) ver 20. Environmental Data Initiative. https://doi.org/10.6073/pasta/5f5fd71e63a76fe2f467dbcd8898d3f7. Accessed 2020
- Viglas JN, Brown CD, Johnstone JF (2013) Age and size effects on seed productivity of northern black spruce. Can J For Res 43:534–543.
- Volney WJA, Fleming RA (2000) Climate change and impacts of boreal forest insects. Agric Ecosyst Environ 82:283–294.
- Walker JX, Mack MC, Johnstone JF (2017) Predicting ecosystem resilience to fire from tree ring analysis in black spruce forests. Ecosystems 20:1137–1150
- Whitman E, Parisien MA, Thompson DK, Flannigan MD (2019) Short-interval wildfire and drought overwhelm boreal forest resilience. Sci Rep 9:1–12.
- Yang Y, Yanai RD, Fatemi FR et al (2015) Sources of variability in tissue chemistry in Northern hardwood species. Can J For Res 46:285–296.

- Zambrano-Bigiarini M, Rojas R (2018) hydroPSO: Particle swarm optimisation, with focus on environmental models. R package version 0.4-1. URL https://cran.r-project.org/package=hydroPSO. https://doi.org/10.5281/zenodo.1287350.
- Zasada JC, Sharik TL, Nygren M (1992) The reproductive process in boreal forest trees. A Systems Analysis of the Global Boreal Forest. pp 85–125
- Zuur AF, Ieno EN, Walker NJ et al (2009) Zero-truncated and zero-inflated models for count data. Mixed effects models and extensions in ecology with R. Springer, New York, pp 261–293

Publisher's Note Springer Nature remains neutral with regard to jurisdictional claims in published maps and institutional affiliations.

Springer Nature or its licensor (e.g. a society or other partner) holds exclusive rights to this article under a publishing agreement with the author(s) or other rightsholder(s); author self-archiving of the accepted manuscript version of this article is solely governed by the terms of such publishing agreement and applicable law.

